Cell

Functional Proteomics Reveals the Biochemical Niche of *C. elegans* DCR-1 in Multiple Small-RNA-Mediated Pathways

Thomas F. Duchaine,[1] James A. Wohlschlegel,[3] Scott Kennedy,[4] Yanxia Bei,[1] Darryl Conte Jr.,[1] KaMing Pang,[1] Daniel R. Brownell,[1] Sandra Harding,[4] Shohei Mitani,[5] Gary Ruvkun,[6] John R. Yates III,[3] and Craig C. Mello[1,2,*]

[1] Program in Molecular Medicine
[2] Howard Hughes Medical Institute
University of Massachusetts Medical School, Worcester, MA 01605, USA
[3] Department of Cell Biology, The Scripps Research Institute, La Jolla, CA 92037, USA
[4] Department of Pharmacology, University of Wisconsin, Madison, WI 53701, USA
[5] Department of Physiology, Tokyo Women's Medical University School of Medicine, Tokyo 162-8666, Japan
[6] Department of Molecular Biology, Massachusetts General Hospital and Department of Genetics, Harvard Medical School, Boston, MA 02114, USA
*Contact: craig.mello@umassmed.edu
DOI 10.1016/j.cell.2005.11.036

SUMMARY

In plants, animals, and fungi, members of the Dicer family of RNase III-related enzymes process double-stranded RNA (dsRNA) to initiate small-RNA-mediated gene-silencing mechanisms. To learn how *C. elegans* Dicer, DCR-1, functions in multiple distinct silencing mechanisms, we used a mass-spectrometry-based proteomics approach to identify DCR-1-interacting proteins. We then generated and characterized deletion alleles for the corresponding genes. The interactors are required for production of three species of small RNA, including (1) small interfering RNAs (siRNAs), derived from exogenous dsRNA triggers (exo-siRNAs); (2) siRNAs derived from endogenous triggers (endo-siRNAs); and (3) developmental regulatory microRNAs (miRNAs). One interactor, the conserved RNA-phosphatase homolog PIR-1, is required for the processing of a putative amplified DCR-1 substrate. Interactors required for endo-siRNA production include ERI-1 and RRF-3, whose loss of function enhances RNAi. Our findings provide a first glimpse at the complex biochemical niche of Dicer and suggest that competition exists between DCR-1-mediated small-RNA pathways.

INTRODUCTION

The use of double-stranded RNA (dsRNA) to induce gene silencing has been termed RNA interference or RNAi (Fire et al., 1998). During RNAi, foreign dsRNAs are processed into small RNAs of approximately 21 nucleotides, termed small interfering RNAs (siRNAs), which guide the destruction of complementary target mRNAs (Mello and Conte, 2004). Natural mechanisms related to RNAi have been implicated in silencing viruses and transposons (Baulcombe, 2004), suggesting that these pathways may function as a form of sequence-directed immunity. RNAi-related mechanisms are also involved in developmental-gene regulation mediated by microRNAs (miRNAs) and in transcriptional silencing and heterochromatin formation (Ambros, 2004; Lippman and Martienssen, 2004).

Central to all RNAi-related gene-silencing phenomena are members of the Dicer family of endoribonucleases. Dicer family members contain several motifs, including double-stranded RNA binding motifs (dsRBMs), ribonuclease III (RNase III) domains, and a DExH-box RNA helicase motif. Dicer processes long double-stranded RNAs and microRNA precursors into small duplex RNA species (Bernstein et al., 2001; Grishok et al., 2001; Hutvagner et al., 2001; Knight and Bass, 2001). These double-stranded Dicer products are unwound, and one of the two strands is preferentially loaded into silencing complexes that mediate downstream functions (Elbashir et al., 2001; Hammond et al., 2001; Martinez et al., 2002). Interestingly, a single Dicer gene is sufficient in many organisms, including humans and *C. elegans*, to mediate dsRNA processing for several distinct small-RNA-guided mechanisms.

The fact that multiple RNAi-related pathways converge on Dicer raises the questions of how specific classes of dsRNA are recognized and recruited by Dicer and of how these distinct trigger-RNA species direct different silencing

Table 1. DCR-1 Interactors and Associated Phenotypes

Name	Structural Description	Phenotype	DCR-1 Purification (Peptide Coverage)
Required for RNAi			
RDE-1	Piwi/PAZ domain	Rde	E (1.4%) W
RDE-4	dsRBD	Rde	E (35%) A[a] (65%) W
DRH-1	DEAH/D box	Rde	E (41%) A (40%) W
DRH-2	DEAH/D box	Rde	E (28%) A (16%) W
Required for RNAi and Development			
T23G7.5 (PIR-1)	RNA phosphatase	Rde, L4 developmental arrest	E (40%) A (41%)
D2005.5 (DRH-3)	DEAH/D box	Rde, early embryonic arrest, sterile	E (29%) A (5%)
ERI Proteins			
W09B6.3 (ERI-3)	Novel (operon and fusion with TAF-6.1)	t.s. sterile, Eri	E (14%) A (17%)
TAF-6.1[b]	TATA-box binding protein-associated factor (operon and fusion with eri-3)	wt (RNAi only)	E (8%) A (8%)
ERI-1	SAP domain, exonuclease	t.s. sterile, Eri	E (13%) W
RRF-3	rdrp	t.s. sterile, Eri	E (23%)
Y38F2AR.1 (ERI-5)	Tudor domain	t.s. sterile, Eri	E (21%)
Required for MicroRNA and Developmental Timing			
ALG-1	Piwi/PAZ domain	Heterochronic	A (7%) W
ALG-2	Piwi/PAZ domain	Heterochronic	A (16%) W
LIN-41	RBCC (NHL family)	Heterochronic, pleiotropic	A (7%)
No Determined Small RNA-Related Functions			
EFT-2	EFT-2 family GTPases	Lethal, pleiotropic	A (13%)
SNR-3	SM domain	Lethal, pleiotropic	A (17%)
F38E11.5	Coatomer (WD repeats)	Lethal, pleiotropic	E (2%)
B0001.2	Domain of unknown function (DUF 272)	wt (RNAi only)	E (6%)
T06A10.3	Conserved	wt (RNAi only)	E (19%)
C32A3.2	Novel	wt	A (30%)

A, gravid adult purification; E: embryonic purification; W, Western detection; rde, required for RNAi; eri, enhancer of RNAi. The mean detected peptide coverage is indicated in parentheses.

[a] A weak peptide coverage of RDE-4 is also detected in the *dcr* nulls, likely due to incomplete counterselection and/or interaction with the residual maternal load.

[b] TAF-6.1 can be expressed as both a single polypeptide and a fusion protein with ERI-3 (see Figure 1 and Discussion). It is unclear at this point whether these proteins interact with DCR-1 separately or as a single polypeptide.

responses. To better understand how DCR-1 carries out its many functions, we undertook a large-scale search for DCR-1-interacting proteins. We show that, in addition to known factors required for the RNAi and miRNA pathways, DCR-1 interactors include novel proteins required for RNAi, chromosome segregation, and the accumulation of several species of endo-siRNA. We show that the DCR-1 interactor and RNA-phosphatase homolog, PIR-1, is required for both siRNA accumulation and the processing of a putative RdRP-derived DCR-1 substrate. At least four interactors, including two previously known proteins, ERI-1 and RRF-3, are required for the accumulation of several endogenous small-RNA species. These findings suggest a role for ERI-1 and RRF-3 in the production of endogenous substrates for DCR-1 and support a model in which specific interactors direct DCR-1 activity toward competing small-RNA-mediated silencing pathways.

RESULTS

A Whole-Animal Search for DCR-1 Interactors

In order to identify DCR-1-associated proteins in *C. elegans*, we affinity purified DCR-1 under native conditions from both

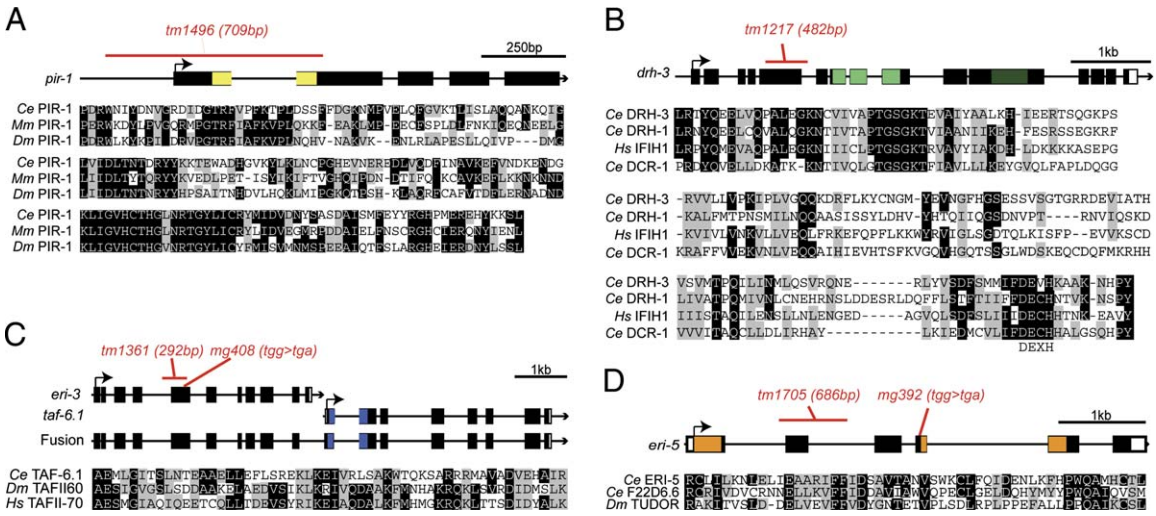

Figure 1. Molecular Structures and Lesions of the *pir-1*, *drh-3*, and *eri* Genes

(A–D) Schematic diagrams showing box/line-exon/intron gene structures for four DCR-1 interactors. The positions of corresponding mutant alleles are indicated in red, and protein alignments of related proteins are provided.

(A) *pir-1* (T23G7.5) encodes a conserved RNA phosphatase. The 709 bp *tm1496* deletion extends from −159 to +550 relative to the ATG and is predicted to remove the entire phosphatase domain (shown in yellow). Protein sequences shown are *C. elegans* PIR-1 (residues 54 to 225), *M. musculus* PIR1 (residues 31 to 198), and *D. melanogaster* CG13197(Dm PIR-1) (residues 6 to 170).

(B) DRH-3 (D2005.5) is a conserved DCR-1-related helicase. Conserved helicase domains are indicated in light and dark green. The 482 bp *tm1217* deletion extends from +892 to +1374, resulting in a premature stop before the helicase domain. Protein sequences shown are DRH-3 (residues 371–516), DRH-1 (293–441), human IFIHI (AAH78180.1, residues 308–454), and *C. elegans* DCR-1 (residues 13–158). The conserved DExH motif is shown beneath the alignment.

(C) *eri-3* (W09B6.3) encodes a novel protein and is expressed in an operon with *TAF-6.1*. An in-frame fusion isoform detected by RT-PCR is shown. The 292 bp *tm1361* deletion removes nucleotides +1357 to +1647, including the splice acceptor site and most of exon 5; *mg408* causes a premature stop also in exon 5. The conserved (TAF) domain of TAF-6.1 is shown in blue. The proteins sequences shown are TAF-6.1 (amino acids 32–85; PF02969), *D. melanogaster* TAFII-60 (CG32211; residues 30–83), and human TAFII-70 (AAN10295.1; residues 30–83).

(D) The *eri-5* gene encodes a protein with two Tudor domains (depicted as orange boxes). The 686 bp *tm1705* deletion extends from +1069 to +1756, including all of exon 2, and is expected to result in out-of-frame splicing from exon 1 to exon 3, causing a premature stop. *mg392* causes a premature stop codon in exon 4. Protein sequences shown include ERI-5 (residues 1–51), its *C. elegans* homolog F22D6.6 (residues 111–161), and *D. melanogaster* Tudor (PF00567, residues 70–119).

embryos and gravid adults (See Experimental Procedures and Figure S1 in the Supplemental Data available with this article online). Fractionation analysis showed that the vast majority of the *C. elegans* DCR-1 protein resides in the soluble fraction obtained from a high-speed centrifugation of total extract (S100 fraction) (Figure S1). We therefore used this S100 fraction, which is enriched for cytoplasmic proteins, as a starting material for further purification.

The purified DCR-1 complexes were eluted and digested into peptides by the sequential addition of Lys-C and trypsin proteases. The peptide mixture was then analyzed using *mul*ti*d*imentional *p*rotein *i*dentification *t*echnology (MudPIT) (Washburn et al., 2001; Wolters et al., 2001). Briefly, MudPIT entails fractionating the peptide sample using multidimensional microscale liquid chromatography, collecting tandem mass spectra for the peptides in the mixture, and identifying the peptide sequence corresponding to each spectrum using the SEQUEST algorithm. The peptide sequences were then used to infer the identities of the protein components of the original mixture. Proteins were considered candidate interactors if they were identified in DCR-1 purifications but not in control purifications. For example, proteins that were recovered in purifications from DCR-1 mutant extracts or from purifications of unrelated proteins were excluded from further analysis. A complete list of proteins identified, including those excluded from further study, is provided in Table S1. A high-confidence set of 20 interactors was compiled based on the criteria of reproducible copurification with DCR-1 when performed with at least two independent immunoaffinity matrices (Table 1). To examine the biological relevance of these interactors, we characterized their loss-of-function phenotypes and their role in small-RNA accumulation and function (see below).

Five interactors were not analyzed further in this study. Three of these, including the translation factor EFT-2, the RNA processing and splicing factor SNR-3/snRNP D1, and the vesicle-transport factor F38E11.5, are associated with extremely pleiotropic loss-of-function phenotypes making it difficult to assign specific roles for these factors in RNAi (Table 1). For two others, T06A10.3 and C32A3.2, we have yet to obtain deletion alleles and have failed to observe any phenotype by RNAi (Table 1). Further studies will be necessary to determine the potential relevance of these five interactors.

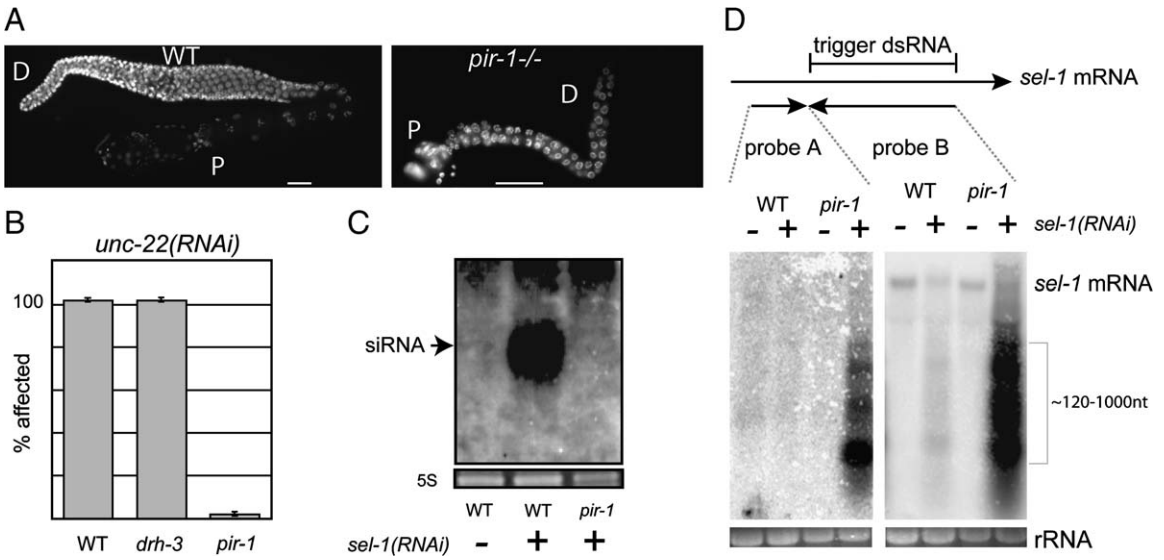

Figure 2. *pir-1* Is an Essential Gene Required for RNAi

(A) Dissected gonads from a wild-type young adult (left panel) and from a terminally arrested *pir-1(tm1496)* animal (right panel) stained with the DNA dye DAPI. Germ nuclei are underproliferated, and mitotic nuclei are absent in the *pir-1* distal (D) germline. Cellularized meiotic germ nuclei are absent in the *pir-1* proximal (P) germline. The scale bar is 10 microns.

(B) Graphical depiction of the sensitivity of wild-type (WT) (n = 44), *drh-3* (n = 45), and *pir-1* (n = 62) animals to feeding RNAi targeting the muscle gene *unc-22*. Error bars represent the 95% confidence interval.

(C) Northern blot analysis of siRNA accumulation in wild-type and *pir-1* animals either with (+) or without (–) exposure to *sel-1(RNAi)* by feeding.

(D) Northern blot analysis of longer *sel-1* RNA species. Probe A (sense orientation) extends 371 nt from the upstream border of the *sel-1(RNAi)* trigger (1155 nt). Probe B (antisense) is directed against the trigger region.

The RNAi Factors RDE-1, RDE-4, and DRH-1/2 Copurify with DCR-1

DCR-1 and the *D*icer-*r*elated *h*elicase DRH-1 were previously shown to copurify with the dsRNA binding protein RDE-4, which is required for the initiation of RNAi (Tabara et al., 2002). We found that RDE-4 and DRH-1, as well as the closely related helicase DRH-2, were recovered in all of the DCR-1 purifications and were among those receiving the highest peptide coverage in purifications from both adult and embryo extracts.

In a previous study, RDE-4 was shown to copurify with the Argonaute protein RDE-1 (Tabara et al., 2002). RDE-1 was consistently and efficiently detected in all of our DCR-1 purifications by Western blot analysis. However, by MudPIT analysis, RDE-1 received a poor peptide coverage (1%) and was only detected in embryonic DCR-1 purifications, suggesting that RDE-1 is present at relatively low abundance in the purification. These findings indicate that other biologically significant proteins may reside among the lower-confidence set of 88 additional interactors (Table S1).

The Interactors PIR-1 and DRH-3 Are Essential Genes Required for RNAi

Two DCR-1 interactors, T23G7.5/PIR-1 and D2005.5/DRH-3, are both highly conserved proteins (see Figures 1A and 1B) and have essential developmental functions. Presumptive null alleles *pir-1(tm1496)* and *drh-3(tm1217)* (Figure 1) exhibit L4 larval arrest and sterile phenotypes, respectively. *pir-1(tm1496)* mutant homozygotes grow normally until the L4 stage but fail to undergo the L4 to adult molt. The resulting arrested larvae are motile and continue to feed for a period of 10 to 12 days but ultimately fail to produce functional gametes and die without progeny (Figure 2A). Interestingly, the cumulative lifespan of *pir-1* homozygotes is approximately equal to that of wild-type animals when measured from the L3 molt. *drh-3* homozygotes are able to reach adulthood but fail to produce functional gametes (see below).

In order to test the *pir-1* and *drh-3* mutants for their sensitivity to RNAi, we allowed homozygous individuals to grow for several days postembryogenesis to allow depletion of maternally loaded wild-type gene products. We then exposed *pir-1* and *drh-3* homozygotes to RNAi targeting the muscle gene *unc-22* and assayed the animals for the characteristic paralyzed twitching phenotype. We found that 100% of the *pir-1* homozygotes exposed to *unc-22* RNAi remain motile, while 100% of wild-type or *drh-3* homozygotes exhibit the characteristic *unc-22* paralyzed twitching phenotype (Figure 2B). To determine whether *pir-1* mutants fail to accumulate siRNAs during RNAi, we exposed wild-type and *pir-1* mutant animals to dsRNA targeting the *sel-1* gene. Wild-type animals exposed to *sel-1(RNAi)* by feeding accumulate abundant *sel-1* siRNAs (Figure 2C), providing a sensitive assay for siRNA detection. We found that *pir-1* mutants failed to accumulate *sel-1* siRNAs (Figure 2C), consistent with a defect in dsRNA processing.

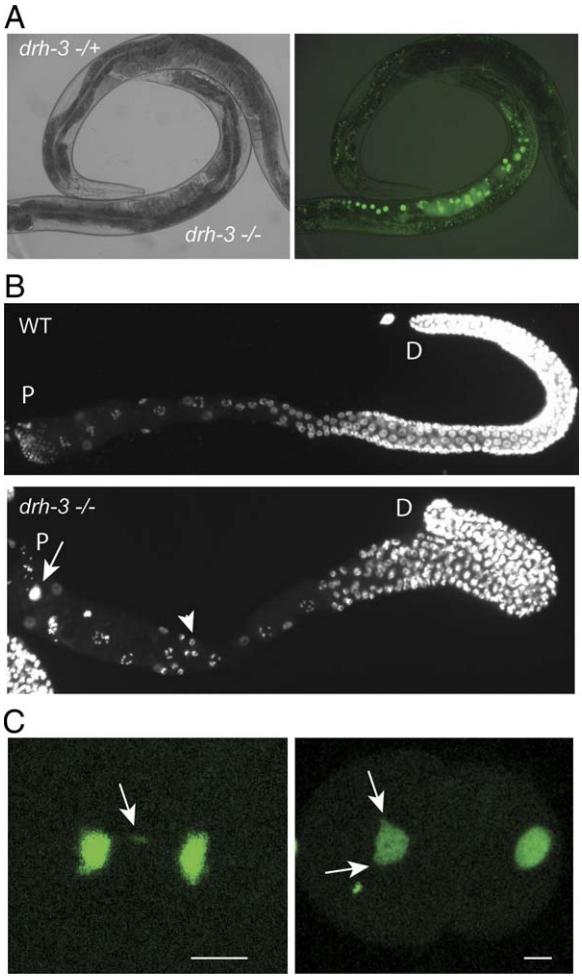

Figure 3. *drh-3* Is an Essential Gene Required for Germline RNAi

(A) DIC and fluorescence images (left and right panels, respectively) after exposure of *pie-1::gfp::h2b* transgenic animals to *gfp* RNAi by feeding. The *drh-3* homozygous animal (indicated) exhibits bright histone GFP expression in the proximal germline and uterus, while the GFP transgene is silenced in the *drh-3* heterozygote.

(B) Dissected gonads from a wild-type young adult (upper panel) and a sterile *drh-3(tm1217)* animal (lower panel) stained with the DNA dye DAPI. Germ nuclei are slightly underproliferated in the *drh-3* distal (D) germline. Sperm (not shown) and cellularized meiotic germ nuclei are present in the *drh-3* proximal (P) germline. An extra row of oocytes often forms in the proximal zone (arrowhead), and endomitotic oocytes are also present (arrow).

(C) Fluorescence images of histone-GFP expression in *pie-1::gfp::h2b* transgenic embryos after *drh-3(RNAi)*. Lagging chromosomes (left panel) and abnormally shaped nuclei (right panel) are indicated by the arrows.

Although siRNAs were absent in *pir-1* mutants, we observed a dramatic accumulation of a higher-molecular-weight RNA species complementary to *sel-1* sense and antisense probes. This RNA species ranged in size from approximately 120 to 500 nucleotides and was only observed in animals exposed to *sel-1* dsRNA (Figure 2D). RNA species of similar size but much lower abundance were also observed in RNA prepared from wild-type worms exposed to *sel-1* dsRNA (Figure 2D, probe B panel, WT *sel-1(RNAi)*+ lane). During RNAi in *C. elegans*, siRNAs accumulate that correspond to the mRNA sequences located 5′ to the trigger dsRNA (Sijen et al., 2001). The accumulation of these siRNAs is thought to reflect DCR-1-mediated processing of amplified dsRNA species. These amplified dsRNA intermediates have not been detected in *C. elegans* but are thought to be produced by cellular RNA-dependent RNA polymerase (RdRP) dependent copying of the target mRNA. To determine whether the RNA species that accumulates in *pir-1* mutants might include products that form during the amplification of RNAi, we probed these RNA blots with sense and antisense *sel-1* probes derived from the region 5′ to the trigger dsRNA. These sense and antisense probes detected a prominent RNA species of approximately 120 nucleotides that is abundant in *pir-1* mutants but is not detected in wild-type animals exposed to *sel-1* dsRNA (Figure 2D, probe A panel and data not shown). Thus *pir-1(+)* activity appears to be required for siRNA accumulation and the DCR-1-mediated processing of an amplified dsRNA intermediate during RNAi.

The finding that *drh-3* homozygotes are sensitive to RNAi targeting the muscle gene *unc-22* (Figure 2B) could reflect either a large maternal load of DRH-3 protein or compensation in somatic tissues by the DRH-1 and DRH-2 paralogs, which were previously shown to be required for both somatic and germline RNAi (Tabara et al., 2002). We therefore asked whether *drh-3(tm1217)* homozygotes are sensitive to RNAi targeting a germline-specific GFP (*pie-1::gfp::h2b*) (Praitis et al., 2001). Homozygous *drh-3(tm1217)* animals and heterozygous siblings were exposed to *gfp* dsRNA as young adults and assayed for GFP expression after 24 hr. The *gfp* reporter was fully silenced in *drh-3* heterozygous animals (Figure 3A). However, *gfp* expression was not diminished in homozygous *drh-3(tm1217)* animals (Figure 3A), suggesting that DRH-3 is required for RNAi, at least in the germline.

In order to gain further insight into the developmental functions of *drh-3*, we examined the germ cells and embryos of *drh-3*-depleted animals (Figures 3B and 3C). The *drh-3(tm1217)* sterile animals exhibit several defects in the proximal region of the gonad, including abnormally aligned and multinucleated germ cells and oocytes that appear to contain excess DNA, perhaps due to endoreduplication (Figure 3B and data not shown). Injection of dsRNA targeting *drh-3* into wild-type L3 or L4 animals induced a sterile phenotype and defects in gametogenesis that were consistent with those observed in the *drh-3(tm1217)* homozygous animals (data not shown). RNAi injections into wild-type adults that had already produced functional gametes resulted in a penetrant embryonic arrest. The earliest visible defects in these *drh-3(RNAi)* embryos occurred during the first cell division and included lagging mitotic chromosomes and anaphase bridges during mitosis (Figure 3C, left panel) and abnormally shaped nuclei during interphase (Figure 3C, right panel). These observations raise the possibility that DRH-3 functions in a small-RNA-mediated process required for proper chromosome segregation.

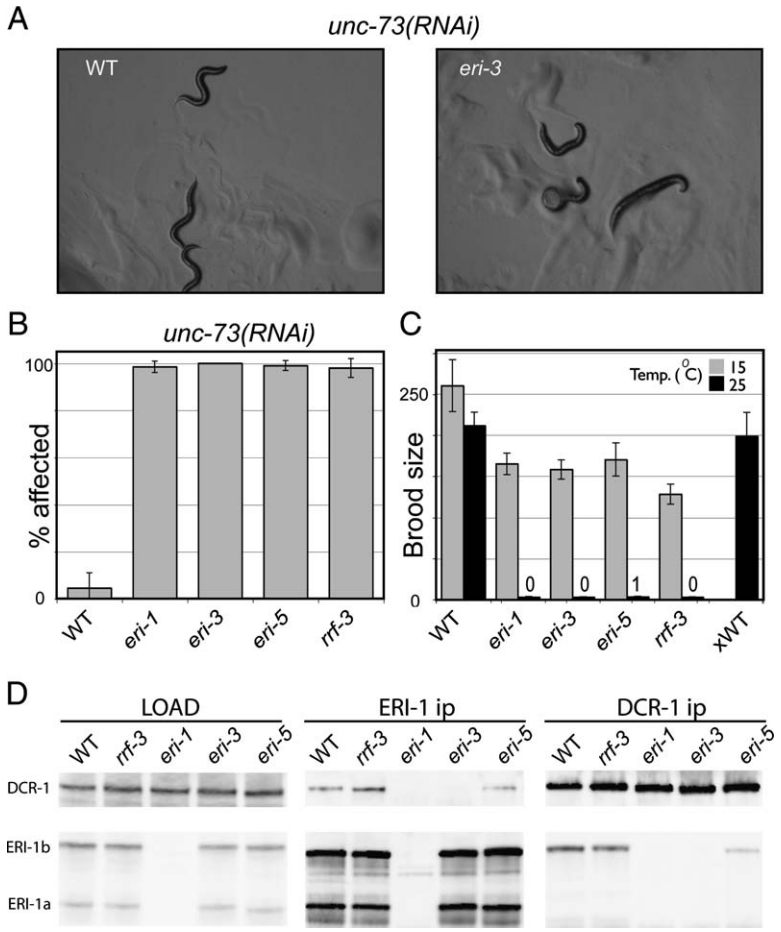

Figure 4. RNAi Enhancement and Developmental Defects of the *eri* Mutants

(A and B) RNAi targeting *unc-73* by feeding induces little or no phenotype in wild-type animals ([A], left panel) but induces a strong uncoordinated phenotype in *eri-3* mutants ([A], right panel) and also in other *eri* mutants as shown in the graphical depiction (B). A total of 200 animals were scored for each genotype.

(C) *eri* mutants exhibit a temperature-sensitive fertility defect. The average brood size for wild-type and *eri* hermaphrodites at 15ºC (light gray) and 25ºC (black) is shown. *xWT* indicates the brood size for *eri-3* animals after mating with N2 males. Error bars in (B) and (C) represent the 95% confidence interval.

(D) ERI-3 and ERI-5 are required for interactions between ERI-1 and DCR-1. ERI-1 and DCR-1 proteins were immunoprecipitated from wild-type, *rrf-3*, *eri-1*, *eri-3*, and *eri-5* mutant embryos, and DCR-1 and ERI-1 (both a and b isoforms) proteins were detected in immunoprecipitates by Western blot.

Three Proteins Required for Developmental Timing Interact with DCR-1

In addition to RDE-1, two other Argonaute proteins, ALG-1 and ALG-2, were found to copurify with DCR-1. These nearly identical proteins have overlapping functions and are required for the efficient processing and function of the miRNAs *lin-4* and *let-7* (Grishok et al., 2001; Ketting et al., 2001) but were not previously known to interact with DCR-1. Surprisingly, the RING-finger B box coiled-coil protein LIN-41 also copurified with DCR-1. LIN-41 is required for the translational repression of LIN-29 in the hypodermis, and LIN-41 itself is regulated by the *let-7* miRNA (Slack et al., 2000). We found that *lin-41(ma104)* homozygotes are sensitive to RNAi and do not exhibit defects in miRNA processing (data not shown). Thus, the physiological significance of the LIN-41-DCR-1 interaction is not known at present.

Mutations in Four DCR-1 Interactors Enhance RNAi

Two genes that encode Dicer interactors, *eri-1* and *rrf-3*, were previously identified as *e*nhancers of *R*NA*i* (*eri*) mutants (Kennedy et al., 2004; Simmer et al., 2002). We therefore looked for enhanced RNAi sensitivity in mutant strains corresponding to other DCR-1 interactors. In addition to analyzing deletion alleles of specific DCR-1 interactors, we also sought new alleles by comparing the physical genetic location of the DCR-1 interactors to the genetic map positions of newly identified but uncloned *eri* mutants. Using this approach, we found that four strains bearing mutations in two additional interactors exhibited enhanced RNAi. These new *eri* alleles define the genes *eri-3* and *eri-5*, which respectively encode a novel protein and a protein with two Tudor domains (Figures 1C and 1D).

In wild-type animals, RNAi targeting *unc-73* results in a low-penetrance-uncoordinated (Unc) phenotype, such that only about 4% of the F1 progeny of animals exposed to *unc-73(RNAi)* exhibit the characteristic deformed, poorly motile phenotype. In contrast, as previously reported, *eri-1(mg366)* and *rrf-3(pk1426)* both exhibit Unc phenotypes when exposed to *unc-73(RNAi)* (Figure 4B). We found that the *eri-3* alleles *tm1361* and *mg408*, and the *eri-5* allele *mg392*, exhibited enhanced RNAi against *unc-73* (Figures 4A and 4B). RNAi targeting *lin-1*, *dpy-13*, *hmr-1*, and a neuronal *unc-47::gfp* was also enhanced in these mutants (data not shown). In addition to the enhanced RNAi phenotype, the *eri* mutant strains exhibit a sperm-defective sterile phenotype at 25ºC, spontaneous silencing of simple transgenic arrays in the soma, and an increase in the frequency of X chromosome nondisjunction resulting in a *h*igh *i*ncidence of *m*ales (Him) phenotype (Figure 4C and data not shown). The *eri-3* gene is located adjacent to a gene encoding

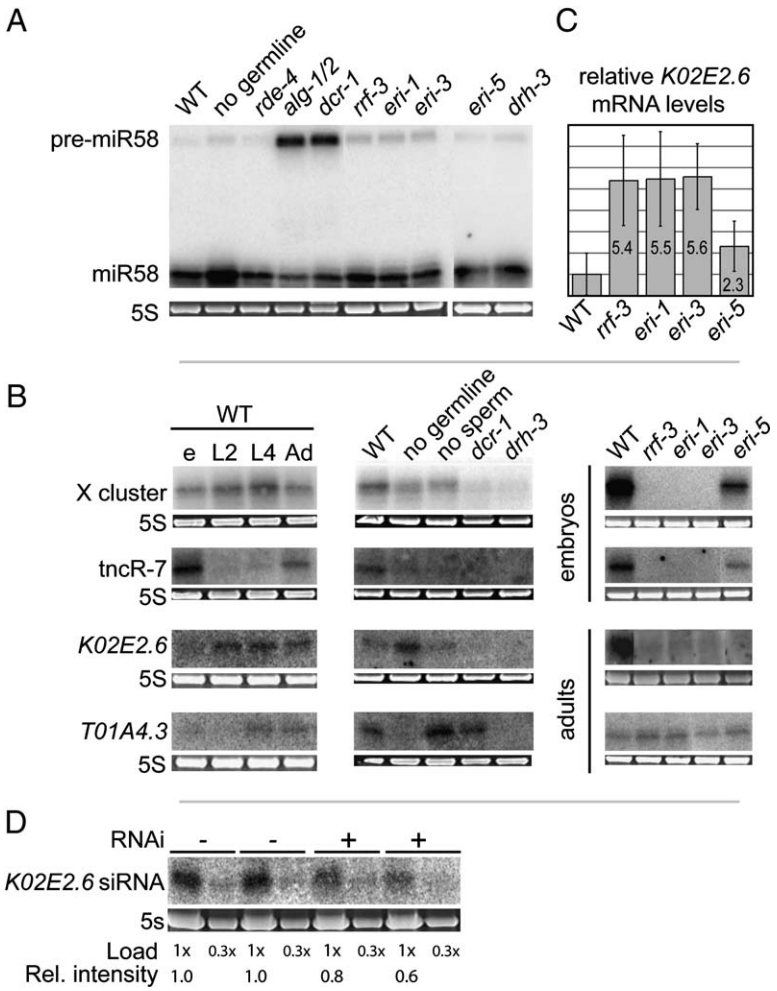

Figure 5. Requirements of DCR-1 Interactors in Small-RNA Biogenesis

(A and B) Northern blot analysis of distinct small-RNA species (as indicated). The 5S ribosomal RNA, visualized by EtBr staining, is shown as a loading control. Populations of *dcr-1* and *drh-3* homozygous animals were prepared by counter-selecting against balancer chromosomes engineered to confer sensitivity to the potent nematicide ivermectin. In (B), the expression profile of each small-RNA species is examined in several stages and tissues: e (embryo), L2, L4, Ad (adult), "no germline" *(glp-4ts)*, and no sperm *(fem-1ts)*. These are compared to RNA isolated from *dcr-1 c.s.* and *drh-3 c.s.* sterile adults, as well as embryos and adults as indicated for the Eri-class mutants.

(C) Real-time PCR analysis of K02E2.6 mRNA levels in the *eri* mutants. The K02E2.6 mRNA levels were normalized to an *Actin* control, and the level of K02E2.6 mRNA was determined relative to wild-type. Error bars show the 95% confidence interval.

(D) Northern analysis of endogenous K02E2.6 siRNA levels in wild-type animals with or without exposure to *sel-1(RNAi)* by feeding. RNA prepared from duplicate independent cultures was examined at two dilutions as indicated. Three independent replicates of this experiment gave similar results (data not shown).

another DCR-1 interacting protein, TAF-6.1, which is a homolog of TAF6, a component of the TFIID and SAGA complexes (Walker et al., 2001). The *taf-6.1* gene appears to be expressed differentially, producing transcripts that include *taf-6.1* alone and longer transcripts that include both *taf-6.1* and *eri-3* (see Figure 1C). Mutations that specifically alter *taf-6.1* have not been identified, and RNAi targeting *taf-6.1* failed to induce a phenotype. Thus, we do not know whether TAF-6.1 itself contributes to the activity of ERI-3 or whether it may have other functions relevant to DCR-1 activity.

The interactions of the ERI-1, ERI-3, ERI-5, and RRF-3 proteins with DCR-1, combined with their similar phenotypes, suggest that they contribute to one or more endogenous functions of DCR-1. To test their possible involvement in a common functional complex, we generated polyclonal antibodies directed against ERI-1 and examined its interaction with DCR-1 by immunoprecipitation in wt animals and in the various *eri* mutants (Figure 4D). Consistent with our MudPIT analysis, we detected ERI-1 in DCR-1 immunoprecipitates and DCR-1 in ERI-1 immunoprecipitates (Figure 4D, WT lanes). Only the long isoform of ERI-1 (ERI-1b) could be detected in DCR-1 immunoprecipitates (Figure 4D, DCR-1 ip panel), suggesting that the two isoforms of ERI-1 may serve distinct molecular functions. The interaction between DCR-1 and ERI-1 was not noticeably affected in extracts prepared from *rrf-3* mutants. However, the interaction was abolished in *eri-3* mutant extracts and was diminished in *eri-5* mutants (*eri-3* and *eri-5* lanes, respectively) (Figure 4D). These observations suggest that the ERI-3 and ERI-5 proteins promote the ERI-1-DCR-1 interaction and strongly support the existence of a common ERI/DCR-1 complex. Furthermore, MudPIT analysis on ERI-1 identifies ERI-3, ERI-5, RRF-3, DCR-1, and DRH-3 (Table S2 and data not shown).

DCR-1 Interactors Exhibit Defects in Small-RNA Accumulation

The diversity of mutant phenotypes associated with DCR-1-interacting proteins suggests that these factors function in distinct cellular or developmental pathways. We reasoned that this phenotypic diversity might be reflected in diverse effects on the expression of specific classes of endogenous small RNAs. A large number of endogenous small RNAs

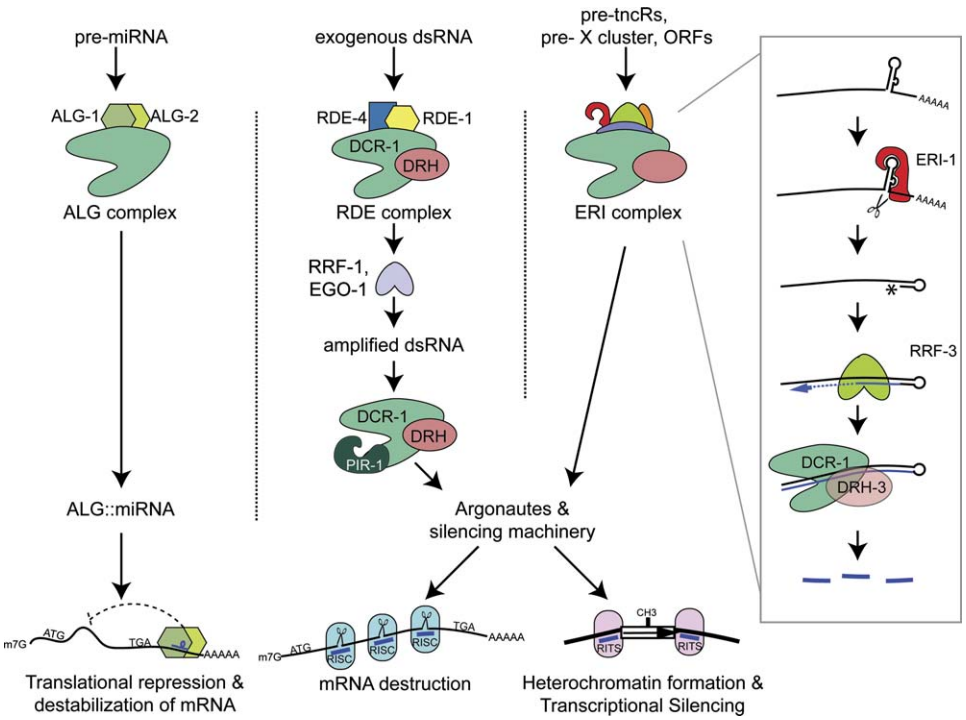

Figure 6. Model for How DCR-1 and Cofactors Initiate Distinct Modes of Silencing

identified in *C. elegans* have been placed into distinct classes that include miRNAs, tiny noncoding RNAs (tncRNAs), a cluster of small RNAs derived from a locus on the X chromosome (X cluster), and finally a group of what appear to be endogenous siRNAs (endo-siRNAs) complementary to predicted protein coding genes (Ambros et al., 2003).

We first asked whether DCR-1 interactors are involved in the biogenesis of miRNAs. Previous work has shown that ALG-1/ALG-2 and DCR-1 are required for the proper maturation of the *lin-4* and *let-7* miRNAs (Grishok et al., 2001). We found that, among the DCR-1-interacting proteins analyzed, only ALG-1 and ALG-2 were required for miRNA formation (Figure 5A). Strains depleted of ALG-1, ALG-2, and DCR-1, but not strains depleted of other DCR-1 interactors, exhibit accumulation of the precursor miRNA species and a concomitant reduction in the amount of the mature miRNA (Figure 5A and data not shown). These data strengthen the idea that the Argonaute proteins ALG-1 and ALG-2 may have a general function along with DCR-1 in the biogenesis of miRNAs.

We next examined the role of DCR-1 and its interactors in the expression of several other small-RNA species, including small RNAs corresponding to the somatically expressed gene K02E2.6, the X cluster, and the tncRNAs (Figure 5B). Accumulation of all of these small-RNA species required DRH-3, DCR-1, and the ERI proteins. However, consistent with its weaker *eri* phenotype, defects in the accumulation of these small-RNA species were also less pronounced in the *eri-5* mutant (Figure 5B and data not shown). This could reflect compensation by its sister gene F22D6.6 (see Figure 1D). Interestingly, *rde-4* was also required for the accumulation of the X cluster small RNAs but was dispensable for the examined tncRNAs and endo-siRNAs (data not shown). The *eri* mutant strains exhibited defects in the accumulation of these small-RNA species even when maintained at the permissive temperature (Figure 5B), suggesting that the failure to produce these siRNA species does not by itself explain the temperature-dependent sperm defect associated with the *eri* mutants.

The accumulation of at least eight small RNAs corresponding to germline-expressed genes, including T01A4.3, required *drh-3* but, surprisingly, did not appear to require DCR-1 or any of the other genes analyzed (Figure 5B and data not shown). This finding could indicate that maternally loaded DCR-1 protein is sufficient to initiate siRNA accumulation for these transcripts.

To determine whether the endo-siRNAs detected here are involved in a silencing mechanism, we asked whether the target mRNA levels are increased in mutants with reduced levels of specific endo-siRNA classes. No corresponding RNA targets are currently known for the X cluster small RNAs or the tncRNAs. However, K02E2.6 is an endogenous somatically expressed mRNA. We therefore used real-time PCR analysis to examine the levels of the K02E2.6 mRNA. We found a 5-fold upregulation of K02E2.6 mRNA levels in the *eri* mutants (Figure 5C), with the exception of *eri-5*, for which a roughly 2-fold increase was observed. These results suggest that the ERI proteins function along with RRF-3,

DRH-3, and DCR-1 as an endogenous gene-silencing machinery.

In *eri-1* and *rrf-3* mutants, the RNAi response to foreign dsRNA is upregulated as are the levels of corresponding exo-siRNAs. While alternative models are possible, this increase in exo-RNAi could reflect competition between the exo- and endo-RNAi pathways for DCR-1 or other limiting factors required for gene silencing. We therefore asked whether the initiation of an exo-RNAi response alters the accumulation of endo-siRNAs. We consistently observed a reduction in endo-siRNA levels in animals exposed to dsRNA targeting the abundantly expressed *sel-1* mRNA (Figure 5D). This reduction in endo-siRNAs was not observed in *rde-1* mutant animals, which are deficient in the initiation of exo-RNAi (data not shown). These findings are consistent with the idea that the ERI-mediated silencing pathway and the exo-RNAi machinery share, and compete for, limiting silencing factors.

DISCUSSION

A Portrait of the Biochemical Niche of DCR-1 in *C. elegans*

The Dicer protein plays a central role in several small-RNA-mediated gene-silencing pathways. In an effort to understand the function and regulation of Dicer, we have performed a large-scale search for proteins that interact with *C. elegans* DCR-1. We have identified interactions between DCR-1 and 20 proteins, 12 of which are linked to DCR-1 activities or its small-RNA products. Two DCR-1 interactors, the RNA phosphatase homolog PIR-1 and the Dicer-related helicase DRH-3, are required for both RNAi and development. Four ERI-class interactors, whose loss of function enhances RNAi, are required for the accumulation of several species of endogenous small RNA, including a class of naturally occurring siRNAs directed against endogenous *C. elegans* genes.

Our findings support a model in which pathway-specific factors guide Dicer in the recognition of its substrates and suggest that the ERI pathway for endogenous gene silencing competes with the exo-RNAi pathway for Dicer or for a limiting pool of downstream silencing effector complexes (Figure 6). In addition to the previously described role for DCR-1 in RNAi and miRNA expression, our findings suggest that DCR-1 and subsets of its binding partners are required for proper chromosome segregation, for production of endogenous small RNAs of unknown function, for silencing endogenous genes, and for a temperature-dependent process required for sperm function.

The ERI Pathway and the Production of Endogenous DCR-1 Substrates

Previous work showing that siRNAs derived from exogenous dsRNA are stabilized in *eri-1* mutants led to the suggestion that ERI-1 might utilize its nuclease domain to degrade siRNAs (Kennedy et al., 2004). However, in light of the findings reported here, new models for ERI-1 function are needed that take into account its interactions with DCR-1 and RRF-3 and explain its role in the production of endo-siRNAs.

One enticing model consistent with these new findings is suggested by the identification of human ERI-1 as an RNA stem-loop binding protein. In addition to its nuclease domain, ERI-1 contains a second domain, called the SAP domain. The SAP domain is thought to contribute to nucleic-acid binding in a variety of chromatin-, DNA-, and RNA-associated proteins (Cheng and Patel, 2004; Dominski et al., 2003). A recent study identified human ERI-1 as a protein that binds, in vitro, to the 6 bp stem-loop structure near the 3′ end of histone mRNAs (Dominski et al., 2003). After binding, the 3′-5′ exonuclease domain of hERI1 catalyzes the removal of the 3′ terminus of the histone mRNA up to the base of the RNA stem loop.

Presently it is not known whether ERI-1 is required for histone mRNA regulation in vivo. However, these findings suggest a general mechanism for how ERI-1 might facilitate the production of dsRNA substrates for DCR-1. Many of the mRNA targets of endo-siRNAs and most tncRNA precursors are not predicted to adopt foldback structures that are sufficiently stable for recognition and processing by DCR-1 (Ambros and Lee, 2004). Instead, shorter stem-loop structures in these RNAs may be recognized by ERI-1. After binding, the exonuclease activity of ERI-1 could then remove any 3′ unpaired nucleotides, creating a hairpin structure suitable for priming the RRF-3-dependent synthesis of longer dsRNA (Figure 6, see box). In this manner, through its interactions with RRF-3 and DCR-1 respectively, ERI-1 could promote the dsRNA synthesis and processing of noncanonical RNA-silencing triggers.

DRH-3 Is an Essential DCR-1 Cofactor

The DRH proteins are members of a conserved helicase family found in diverse organisms ranging from archaea to humans. These genes have the distinction of encoding helicase domains that are most closely related to the helicase domain of Dicer. Interestingly, mammalian members of this family are activated transcriptionally in response to viral infection and appear to play a role in dsRNA-induced signal transduction in innate immunity (Yoneyama et al., 2004). The close interaction of all three *C. elegans* DRH proteins with DCR-1 raises the question of whether their mammalian homologs may also interact with Dicer. If so, it will be interesting to examine whether these DRH homologs function with Dicer in a sequence-directed form of innate immunity in vertebrate cells.

DRH-3 is essential for viability but is not required for the processing of any of several miRNA gene products examined in this study. Instead, we have found that DRH-3 is required for RNAi in the germline and for the production of several classes of endogenous small RNAs of unknown function. In addition, DRH-3 appears to have a role in promoting chromosome segregation. RNAi-related mechanisms have been linked to chromosome segregation in yeast, tetrahymena, flies, and vertebrates (Fukagawa et al., 2004; Mochizuki et al., 2002; Provost et al., 2002; Volpe et al., 2002, 2003). In fission yeast, Dicer has been

implicated in silencing of kinetochore-associated repetitive genes and is thought to be required for the assembly of chromatin domains that promote faithful chromosome segregation (Volpe et al., 2002, 2003). Thus, DRH-3 may function along with DCR-1 in a similar process required for chromosome segregation in *C. elegans*.

DRH-3 is required along with the ERI-class proteins in the production of several species of endogenous small RNA. The small-RNA species absent in the *eri* mutants represent only a subset of the small-RNA species that disappear in *drh-3* mutants. These findings could explain why *drh-3* mutants are completely sterile and exhibit defects in germline proliferation and gametogenesis, while *eri* mutants exhibit a less severe fertility defect that primarily affects sperm function. Conceivably, DRH-3 and the ERI proteins function with DCR-1 to produce small RNAs that mediate chromatin compaction and other functions required for fertility and chromosome segregation. Important insights into these mechanisms will likely come from identifying the RNA species that reside in, or are processed by, the ERI and DRH complexes.

A RNA-Phosphatase Homolog Required for RNAi

The PIR-1 protein interacts with Dicer in both embryos and adults and, like Dicer, appears to be essential for both development and RNAi. Animals homozygous for a presumptive null allele of *pir-1(tm1496)* are viable but arrest development as L4 stage larvae. Remarkably, these arrested animals are healthy and exhibit a nearly normal lifespan of 12 to 15 days. These findings suggest that the *pir-1* homozygotes are not deficient in general functions required for the completion of development. Rather, *pir-1* mutants may terminate development prematurely as a result of defects in one or more small-RNA-mediated mechanisms. Previous reports have demonstrated a role for the microRNAs *lin-4* and *let-7* in the regulation of larval development, and DCR-1 is required for proper *lin-4* and *let-7* expression. However, our experiments to date have failed to link PIR-1 to the accumulation of miRNAs or other endogenous small-RNA species.

During RNAi in several species, including *C. elegans*, plants, and fungi, the target mRNA is thought to serve as a template for the production of secondary dsRNAs that are processed by Dicer to amplify the silencing signal. Compelling evidence supporting this mechanism in *C. elegans* comes from the detection of siRNAs derived from sequences 5′ to the original trigger dsRNA (Sijen et al., 2001). However, the amplified putative Dicer substrate has not been detected in previous studies. The findings reported here are consistent with the possible accumulation of this dsRNA intermediate in *pir-1* mutant animals. We have shown that *pir-1* mutants accumulate abundant 120 nucleotide RNA species, as well as larger RNA species consisting of both sense and antisense strands, and that this accumulated RNA includes sequences upstream of the trigger dsRNA. These findings raise the possibility that amplified dsRNA species cannot be processed by DCR-1 in the absence of PIR-1 activity. Together with the finding that PIR-1 interacts physically with DCR-1, these results support a model in which PIR-1 is not required for the initial round of dicing on the trigger dsRNA but rather is required to prepare amplified dsRNA intermediates for processing by DCR-1 (Figure 6).

The vertebrate homolog of PIR-1 associates with RNP particles in mammalian cells (Deshpande et al., 1999; Yuan et al., 1998) and exhibits specificity toward removal of 5′ γ- and β-phosphates from RNA triphosphate substrates. In this respect, vertebrate PIR-1 is functionally similar to its closely related homologs required for removal of the γ-phosphate prior to mRNA capping. Amplification of RNAi could involve a primer-independent RNA-dependent RNA polymerase reaction that may result in dsRNA substrates with 5′ triphosphates. If so, it is possible that PIR-1 processes these substrates to generate optimal 5′ monophosphate products for recognition by DCR-1 or Argonaute proteins involved in downstream silencing.

In summary, findings from this whole-organism proteomics study identify surprising new factors that interact with DCR-1 and are required for its functions. Our findings demonstrate that Dicer's distinct small-RNA-mediated pathways influence one another and may compete for DCR-1 or other limiting downstream factors. Several of the DCR-1 interactors identified, including PIR-1 and ERI-1, are highly conserved. It will now be important to gain further insights into the specific biochemical functions of these proteins and to learn whether their functions and interactions with Dicer are conserved in other organisms.

EXPERIMENTAL PROCEDURES

C. elegans Genetics and Culture

The Bristol strain N2 was used as the standard wild-type strain. Alleles, marker mutations, and balancer chromosomes used are listed by chromosome as follows: *LGI*: *avr-14(ad1302)*, *drh-3(tm1217)*, *lin-41(ma104)*, *glp-4(bn2)*, *hT2[qIs48] (I;III)*; *LGII*: *alg-2(ok304)*, *pir-1(tm1496)*, *rrf-3(pk1426)*, *eri-3(tm1361)*, *eri-3(mg408)*; *LGIII*: *dcr-1(ok247)*, *dpy-17(e164)*, *rde-4(ne337)*, *qC1[nels(myo-2::avr-15, rol-6, unc-22(RNAi))]*; *LGIV*: *fem-1(e1965)*, *eri-1(mg366)*, *eri-5(mg392)*, *eri-5 (tm1705)*; *LGV*: *avr-15(ad1051)*, *glc-1(pk54::Tc1)*. *C. elegans* culture and genetics were as described in Brenner (1974). RNAi was carried out as previously reported (Fire et al., 1998; Timmons et al., 2001).

The deletion mutations were induced by a combination of TMP chemical mutagen and UV treatment and were identified by detection of a PCR product length polymorphism, as previously reported (Gengyo-Ando and Mitani, 2000).

The *pir-1* and *drh-3* deletion strain was outcrossed five times, and the chromosome arms were broken by recombination to remove unlinked mutations. A *myo-3* promoter-driven *pir-1* cDNA transgene partially restores RNAi sensitivity in body muscle, indicating that the *pir-1* mutation is responsible for the loss-of-RNAi phenotype. The *drh-3* mutant was rescued using a yeast artificial chromosome (Y74D9) containing the *drh-3* locus.

DCR-1 Antibodies and Tagged Transgenes

Rabbit antisera against DCR-1 residues 1145 to 1347 in the pCal-KC vector (Stratagene) were affinity purified, dialyzed against PBS/5% glycerol, concentrated to ~1 μg/μl, and stored frozen at −80ºC. An 8×HA-DCR-1 rescuing transgene was constructed in a yeast artificial chromosome (YAC) by homologous recombination as described previously (Rocheleau et al., 1999). Total QIAGEN purified genomic yeast DNA including the engineered DCR-1 YAC was injected at 200 ng/μl along with 50 ng/μl of a *sqt-3::gfp* marker plasmid to generate the rescued strain WM82.

C. elegans Preparations

Synchronous populations of young adults were harvested, rinsed two times in M9, floated on sucrose, rinsed two times in M9, and then incubated with rocking in M9 for 30 min at RT to allow digestion of the gut bacterial load. For embryonic preparations, gravid adults were treated with hypochlorite, and the embryos were rinsed three times in M9 and two times in cold water. Concentrated pellets of adults and embryos were stored at −80ºC until needed. Samples were suspended on ice in one volume of hypotonic buffer (10 mM HEPES-KOH [pH 7.5], 10 mM KOAc, 2 mM $Mg(OAc)_2$, 1 mM DTT) with 4× concentration Complete protease inhibitors (Roche) and homogenized in a stainless-steel Dounce homogenizer for 20–30 strokes on ice. The resulting slurry was transferred to an Eppendorf tube, adjusted to 110 mM KCl (isotonic condition), vortexed, and allowed to sit on ice for 10 min. The supernatant from a short 1500 × g centrifugation was further clarified twice at 10,000 × g for 10 min at 4ºC. The resulting supernatant was then loaded in a polyallomer Beckman microfuge tube and centrifuged at 100,000 × g for 1 hr at 4ºC in a TLA100.3 (Beckman Instruments) to yield the S100.

Matrix Preparation and Immunoprecipitations

For typical preparations, 1 mg of DCR-1 affinity-purified polyclonal antibodies was covalently coupled to 200 μl rProtA beads (Pierce) using DMP. Agarose-coupled matrixes from monoclonal HA-7 (Sigma) and high-affinity monoclonal 3F10 (Roche) were used for embryonic purifications. Prior to adding the matrixes, the S100 fraction was further quantified and diluted to 5 mg/ml concentration in 1% Triton X-100-supplemented isotonic buffer (50 μl bead slurry was added for 2 ml IP volume). Each experiment was carried out in duplicate or triplicate from independent worm preparations.

Immunoprecipitations were carried out at 4ºC for 1 hr, and beads were then washed three times in the immunoprecipitation buffer. Beads were then treated with 20 μg/ml RNase A for 30 min on ice in the same buffer, then washed three more times. The beads were washed one more time in cold PBS, and all the supernatant was drained. Bound proteins were eluted in 8 M urea/50 mM HEPES (pH 7.5) and were acetone precipitated. A fraction of the elution was monitored by SDS-PAGE and silver stain. For adult purifications, controls included preparations from a *dcr-1* deletion allele (Figure S1B) and a mock purification with the neutralized affinity beads. For embryonic purifications, controls included nontransgenic N2 embryos (Figure S1C and data not shown).

Multidimensional Protein Identification

Acetone precipitates from the DCR-1 and control purifications were resuspended in digestion buffer (8 M urea, 100 mM Tris-HCl [pH 8.5]) and digested by the sequential addition of Lys-C and trypsin proteases as previously described (McDonald et al., 2002). The digests were then analyzed by μLC/μLC-MS/MS using a Finnigan LCQ Deca ion trap mass spectrometer. Multidimensional chromatography was performed online according to MacCoss et al. (2002). Tandem mass spectra were collected in data-dependent fashion by collecting one full MS scan (m/z range = 400–1400) followed by MS/MS spectra of the three most abundant precursor ions. The collection of resulting spectra was then searched against a database of *C. elegans* ORFs obtained from Wormbase using the SEQUEST algorithm (Eng et al., 1994). Peptide identifications were organized and filtered using the DTASelect program (Tabb et al., 2002). Filtering criteria for positive protein identifications were the identification of two unique, half, or fully tryptic peptides with Xcorr values greater than 1.8 for +1 spectra, 2.5 for +2 spectra, and 3.5 for +3 spectra and a ΔCn value greater than 0.08.

RNA Preparation and Northern Analysis

Total RNA was prepared using the TRI Reagent method (MRC, Inc.). Small-RNA species were enriched using the mirVana kit (Ambion). Five to ten micrograms of small RNA was resolved per lane of a 15% UREA-TBE gel and transferred to either Hybond N+ (Amersham Biosciences) or Zeta-probe GT (Bio-Rad). Membranes were hybridized with ^{32}P-labeled Starfire (IDT) probes in Ultrahyb Oligo buffer (Ambion).

Real-Time PCR

Real-time PCR was performed using the Bio-Rad iScript cDNA synthesis kit and SYBR Green Supermix according to the supplier's instructions. Oligo pairs used in this study were *k02e2.6*, GCCCTACCGAAATGTTGT TGG and AAGGCACCTGGTCCGTCCATAAAC; *GAPDH*, TGGAGCCGA CTATGTCGTTGAG and GCAGATGGAGCAGAGATGATGAC.

Imaging and Video Microscopy

DIC and fluorescence images were collected using a Hamamatsu Orca-ER digital camera mounted on a Zeiss Axioplan 2 microscope. Time-lapse video microscopy was performed using a Leica TCS SP2 confocal microscope system.

Supplemental Data

Supplemental Data include two tables and one figure and can be found with this article online at http://www.cell.com/cgi/content/full/124/2/343/DC1/.

ACKNOWLEDGMENTS

We thank Victor Ambros for sharing key unpublished observations. We thank James F. Mello, Chun-Chieh Chen, and Julie Claycomb for useful comments on the manuscript. Some nematode strains were provided by the Caenorhabditis Genetics Center (CGC). We thank the Sanger Institute for providing a YAC clone used in this work. T.F.D. is a postdoctoral fellow of the Canadian Institutes of Health Research (CIHR). C.C.M. is a Howard Hughes Medical Institute Investigator. This work was funded in part by the National Institutes of Health (GM58800).

Received: July 13, 2005
Revised: October 3, 2005
Accepted: November 7, 2005
Published: January 26, 2006

REFERENCES

Ambros, V. (2004). The functions of animal microRNAs. Nature *431*, 350–355.

Ambros, V., and Lee, R.C. (2004). Identification of microRNAs and other tiny noncoding RNAs by cDNA cloning. Methods Mol. Biol. *265*, 131–158.

Ambros, V., Lee, R.C., Lavanway, A., Williams, P.T., and Jewell, D. (2003). MicroRNAs and other tiny endogenous RNAs in C. elegans. Curr. Biol. *13*, 807–818.

Baulcombe, D. (2004). RNA silencing in plants. Nature *431*, 356–363.

Bernstein, E., Caudy, A.A., Hammond, S.M., and Hannon, G.J. (2001). Role for a bidentate ribonuclease in the initiation step of RNA interference. Nature *409*, 363–366.

Brenner, S. (1974). The genetics of Caenorhabditis elegans. Genetics *77*, 71–94.

Cheng, Y., and Patel, D.J. (2004). Crystallographic structure of the nuclease domain of 3′hExo, a DEDDh family member, bound to rAMP. J. Mol. Biol. *343*, 305–312.

Deshpande, T., Takagi, T., Hao, L., Buratowski, S., and Charbonneau, H. (1999). Human PIR1 of the protein-tyrosine phosphatase superfamily has RNA 5′-triphosphatase and diphosphatase activities. J. Biol. Chem. *274*, 16590–16594.

Dominski, Z., Yang, X.C., Kaygun, H., Dadlez, M., and Marzluff, W.F. (2003). A 3′ exonuclease that specifically interacts with the 3′ end of histone mRNA. Mol. Cell *12*, 295–305.

Elbashir, S.M., Lendeckel, W., and Tuschl, T. (2001). RNA interference is mediated by 21- and 22-nucleotide RNAs. Genes Dev. *15*, 188–200.

Eng, J.K., McCormack, A.L., and Yates, J.R., 3rd. (1994). An approach to correlate tandem mass spectral data of peptides with amino acid sequences in a protein database. J. Am. Soc. Mass Spectrom. *5*, 976–989.

Fire, A., Xu, S., Montgomery, M.K., Kostas, S.A., Driver, S.E., and Mello, C.C. (1998). Potent and specific genetic interference by double-stranded RNA in Caenorhabditis elegans. Nature *391*, 806–811.

Fukagawa, T., Nogami, M., Yoshikawa, M., Ikeno, M., Okazaki, T., Takami, Y., Nakayama, T., and Oshimura, M. (2004). Dicer is essential for formation of the heterochromatin structure in vertebrate cells. Nat. Cell Biol. *6*, 784–791.

Gengyo-Ando, K., and Mitani, S. (2000). Characterization of mutations induced by ethyl methanesulfonate, UV, and trimethylpsoralen in the nematode Caenorhabditis elegans. Biochem. Biophys. Res. Commun. *269*, 64–69.

Grishok, A., Pasquinelli, A.E., Conte, D., Li, N., Parrish, S., Ha, I., Baillie, D.L., Fire, A., Ruvkun, G., and Mello, C.C. (2001). Genes and mechanisms related to RNA interference regulate expression of the small temporal RNAs that control C. elegans developmental timing. Cell *106*, 23–34.

Hammond, S.M., Boettcher, S., Caudy, A.A., Kobayashi, R., and Hannon, G.J. (2001). Argonaute2, a link between genetic and biochemical analyses of RNAi. Science *293*, 1146–1150.

Hutvagner, G., McLachlan, J., Pasquinelli, A.E., Balint, E., Tuschl, T., and Zamore, P.D. (2001). A cellular function for the RNA-interference enzyme Dicer in the maturation of the let-7 small temporal RNA. Science *293*, 834–838.

Kennedy, S., Wang, D., and Ruvkun, G. (2004). A conserved siRNA-degrading RNase negatively regulates RNA interference in C. elegans. Nature *427*, 645–649.

Ketting, R.F., Fischer, S.E., Bernstein, E., Sijen, T., Hannon, G.J., and Plasterk, R.H. (2001). Dicer functions in RNA interference and in synthesis of small RNA involved in developmental timing in C. elegans. Genes Dev. *15*, 2654–2659.

Knight, S.W., and Bass, B.L. (2001). A role for the RNase III enzyme DCR-1 in RNA interference and germ line development in Caenorhabditis elegans. Science *293*, 2269–2271.

Lippman, Z., and Martienssen, R. (2004). The role of RNA interference in heterochromatic silencing. Nature *431*, 364–370.

MacCoss, M.J., McDonald, W.H., Saraf, A., Sadygov, R., Clark, J.M., Tasto, J.J., Gould, K.L., Wolters, D., Washburn, M., Weiss, A., et al. (2002). Shotgun identification of protein modifications from protein complexes and lens tissue. Proc. Natl. Acad. Sci. USA *99*, 7900–7905.

Martinez, J., Patkaniowska, A., Urlaub, H., Luhrmann, R., and Tuschl, T. (2002). Single-stranded antisense siRNAs guide target RNA cleavage in RNAi. Cell *110*, 563–574.

McDonald, W.H., Ohi, R., Miyamoto, D.T., Mitchison, T.J., and Yates, J.R., 3rd. (2002). Comparison of three directly coupled HPLC MS/MS strategies for identification of proteins from complex mixtures: single-dimension LC-MS/MS, 2-phase MudPIT, and 3-phase MudPIT. Int. J. Mass Spectrom. *219*, 245–251.

Mello, C.C., and Conte, D., Jr. (2004). Revealing the world of RNA interference. Nature *431*, 338–342.

Mochizuki, K., Fine, N.A., Fujisawa, T., and Gorovsky, M.A. (2002). Analysis of a piwi-related gene implicates small RNAs in genome rearrangement in tetrahymena. Cell *110*, 689–699.

Praitis, V., Casey, E., Collar, D., and Austin, J. (2001). Creation of low-copy integrated transgenic lines in Caenorhabditis elegans. Genetics *157*, 1217–1226.

Provost, P., Silverstein, R.A., Dishart, D., Walfridsson, J., Djupedal, I., Kniola, B., Wright, A., Samuelsson, B., Radmark, O., and Ekwall, K. (2002). Dicer is required for chromosome segregation and gene silencing in fission yeast cells. Proc. Natl. Acad. Sci. USA *99*, 16648–16653.

Rocheleau, C.E., Yasuda, J., Shin, T.H., Lin, R., Sawa, H., Okano, H., Priess, J.R., Davis, R.J., and Mello, C.C. (1999). WRM-1 activates the LIT-1 protein kinase to transduce anterior/posterior polarity signals in C. elegans. Cell *97*, 717–726.

Sijen, T., Fleenor, J., Simmer, F., Thijssen, K.L., Parrish, S., Timmons, L., Plasterk, R.H., and Fire, A. (2001). On the role of RNA amplification in dsRNA-triggered gene silencing. Cell *107*, 465–476.

Simmer, F., Tijsterman, M., Parrish, S., Koushika, S.P., Nonet, M.L., Fire, A., Ahringer, J., and Plasterk, R.H. (2002). Loss of the putative RNA-directed RNA polymerase RRF-3 makes C. elegans hypersensitive to RNAi. Curr. Biol. *12*, 1317–1319.

Slack, F.J., Basson, M., Liu, Z., Ambros, V., Horvitz, H.R., and Ruvkun, G. (2000). The lin-41 RBCC gene acts in the C. elegans heterochronic pathway between the let-7 regulatory RNA and the LIN-29 transcription factor. Mol. Cell *5*, 659–669.

Tabara, H., Yigit, E., Siomi, H., and Mello, C.C. (2002). The dsRNA binding protein RDE-4 interacts in vivo with RDE-1, DCR-1, and a conserved DExH-box helicase to direct RNA interference in C. elegans. Cell *109*, 861–871.

Tabb, D.L., McDonald, W.H., and Yates, J.R., 3rd. (2002). DTASelect and Contrast: tools for assembling and comparing protein identifications from shotgun proteomics. J. Proteome Res. *1*, 21–26.

Timmons, L., Court, D.L., and Fire, A. (2001). Ingestion of bacterially expressed dsRNAs can produce specific and potent genetic interference in Caenorhabditis elegans. Gene *263*, 103–112.

Volpe, T., Schramke, V., Hamilton, G.L., White, S.A., Teng, G., Martienssen, R.A., and Allshire, R.C. (2003). RNA interference is required for normal centromere function in fission yeast. Chromosome Res. *11*, 137–146.

Volpe, T.A., Kidner, C., Hall, I.M., Teng, G., Grewal, S.I., and Martienssen, R.A. (2002). Regulation of heterochromatic silencing and histone H3 lysine-9 methylation by RNAi. Science *297*, 1833–1837.

Walker, A.K., Rothman, J.H., Shi, Y., and Blackwell, T.K. (2001). Distinct requirements for C.elegans TAF(II)s in early embryonic transcription. EMBO J. *20*, 5269–5279.

Washburn, M.P., Wolters, D., and Yates, J.R., 3rd. (2001). Large-scale analysis of the yeast proteome by multidimensional protein identification technology. Nat. Biotechnol. *19*, 242–247.

Wolters, D.A., Washburn, M.P., and Yates, J.R., 3rd. (2001). An automated multidimensional protein identification technology for shotgun proteomics. Anal. Chem. *73*, 5683–5690.

Yoneyama, M., Kikuchi, M., Natsukawa, T., Shinobu, N., Imaizumi, T., Miyagishi, M., Taira, K., Akira, S., and Fujita, T. (2004). The RNA helicase RIG-I has an essential function in double-stranded RNA-induced innate antiviral responses. Nat. Immunol. *5*, 730–737.

Yuan, Y., Li, D.M., and Sun, H. (1998). PIR1, a novel phosphatase that exhibits high affinity to RNA . ribonucleoprotein complexes. J. Biol. Chem. *273*, 20347–20353.